13th International Symposium on Particle Image Velocimetry – ISPIV 2019
Munich, Germany, July 22-24, 2019

Flow structure and combustion in an impinging jet with swirl studied simultaneously by stereo PIV, OH PLIF and HCHO PLIF

Roman Tolstoguzov[1,2], Dmitriy Sharaborin[1,2], Dmitriy Markovich[1,2],

Vladimir Dulin[1,2]*

[1]Kutateladze Institute of Thermophysics, Siberian Branch of the Russian Academy of Sciences, Novosibirsk, Russia

[2] Novosibirsk State University, Novosibirsk, Russia

* vmd@itp.nsc.ru

Abstract

The present paper reports on an experimental study of flow structure and coherent structures in impinging jets with strong swirl and combustion of lean propane/air mixture by a combined application of OH PLIF, HCHO PLIF and PIV. To reveal coherent structures, the experimental data are processed by proper orthogonal decomposition (POD). The decomposition has revealed two kinds of large-scale organized flow structures. One kind corresponds to vortex structures formed in mixing layers of the swirling jets and causing deformations of the combustion zone. Another corresponds to large-scale flow oscillations during jet impingement onto the surface, which are found to be statistically correlated with fluctuations of HCHO fluorescence intensity inside the recirculation zone.

1 Introduction

One of the flow configurations, where combustion takes place near walls, is a jet-flame impinging on an obstacle. In particular, impinging jet-flames are used for intensive heating of solid materials. Local heat transfer conditions are determined by the flow structure and dynamics and by efficiency of fuel combustion upstream the obstacle. Flow swirl is often organized to intensify combustion in jets. It provides successive ignition and stable combustion (without blow-off) near the nozzle exit for a wide range of flow rates of fuel and oxidizer. Organization of flow with strong swirl usually results in breakdown of the swirling jet's vortex core with formation of a central recirculation zone and intensive velocity fluctuations near the nozzle (Billant et al. 1998, Oberleithner et al. 2011). This features lead to intensification of heat and mass transfer and provide favorable conditions for efficient fuel combustion in a compact volume (Syred and Beer 1974, Gupta et al. 1984, Weber and Dugué 1992), which allows design of compact heaters.

At the same time, as reported in a number of papers, swirl induces unsteady flow dynamics, which may interfere with unsteady combustion modes. Most of the published experimental studies of impinging jet-flames with combustion, including few works on turbulent jet-flames with swirl, reports on temperature and heat flux distributions on the impinging surface (Luo et al. 2010, Singh et al. 2012, Chander and Singh 2013, Singh and Chander 2013, Singh et al. 2014). Thus, currently there

is a lack of experimental studies on flow structure in impinging jets with swirl and combustion. Detailed information on spatial structure of turbulent flows with combustion can be obtained by using modern optical methods, which are often used for diagnostics of combustion in near-wall flows (Dreizler and Böhm 2015). Pointwise laser Doppler velocimetry technique provides local flow velocity (Edwards et al. 1993, Cheng 1995, Hassel and Linow 2000). Measurements of local Rayleigh scattering, spontaneous Raman scattering (SRS), coherent anti-Stokes Raman scattering (CARS) or laser-induced fluorescence (LIF) provides pointwise and planar (2D) information on gas temperature and species concentration, flame front location and regions of intensive heat release (Kohse-Höinghaus 1994, Hassel and Linow 2000, Miles et al. 2000, Sharaborin et al. 2018).

Simultaneous registration of planar LIF (PLIF) of OH* (hydroxyl radical) and HCHO (formaldehyde) has been used successfully for detection of regions with intensive local heat release in premixed hydrocarbon flames (Fayoux et al. 2005, Kariuki et al. 2015). In particular, Röder et al. (2012) have performed OH and HCHO PLIF measurements for detection of local heat release zones in a lean methane/air swirling flame. Recently, validation of OH and HCHO PLIF measurements of local heat release for a premixed laminar conical flame has been provided by Mulla et al. (2016). Particle image velocimetry (PIV) technique is often used for planar velocity measurement in gaseous flows, including flows with combustion (Stella et al. 2001, Johnson et al. 2005, Cheng et al. 2008, Korobeinichev et al. 2014). Moreover, PIV is often combined with PLIF methods for multi-parameter measurements in the same plane.

The present work focuses on the experimental study of flow structure and coherent structures in impinging jets with strong swirl and premixed combustion by a combined application of OH PLIF, HCHO PLIF and PIV. To reveal coherent structures, the PIV data were processed by proper orthogonal decomposition (POD) (Sirovich 1987). The PLIF snapshots were phase-averaged according to the temporal coefficients of the POD modes.

2 Experimental setup

The jet flow was produced by a swirl burner, oriented vertically, and impinged normally on a flat metallic plate. The burner consisted of an axisymmetric contraction nozzle with a vane swirler mounted inside (similar to Alekseenko et al. 2007). By using two swirlers with different inclination angles of blades, two swirl rates S were studied, viz. below (S = 0.41) and above (S = 1.0) critical value (≈0.6) for the vortex breakdown for non-reacting swirling jet unconfined conditions. The swirl rates were estimated based on the geometrical parameters of the swirlers (Gupta et al. 1984):

$$S = \frac{2}{3}\left(\frac{1-\left(d_1/d_2\right)^3}{1-\left(d_1/d_2\right)^2} \right)\tan\left(\psi\right) \qquad (1)$$

Here d_1 = 7 mm is the diameter of the centerbody supporting the vanes, d_2 = 27 mm is the external diameter of the swirler, and ψ=55° is the vanes inclination angle relatively to the axis.

The impinged plate represented bottom of a steel cylindrical tank (with the diameter of 300 mm) installed above the nozzle. The surface temperature was kept constant by water, circulated inside the tank, with temperature of 96 °C. The distance between the nozzle and the impingement plate was changed by moving the burner, mounted on a coordinate system, with a positioning accuracy of 0.1

mm. Flow cases with nozzle-to-plate distance H equal to$3d$ and $1d$ were investigated, as well as the unconfined flame configuration. Flow rates of the fuel (propane) and air were controlled by mass flow meters (Bronkhorst). The equivalence ratio of the mixture issued from the nozzle was 0.7. The Reynolds number of the jet determined by the bulk velocity of the air flow (U_0 = 5 m/s), nozzle exit diameter (d = 15 mm) and the viscosity of air was Re = 5 000. To provide PIV measurements, the air flow was seeded by TiO_2 particles with the mean size of approximately 0.5 μm.

The used stereoscopic PIV system included pair of CCD cameras (Bobcat IGV-B2020, 4 Mpix, 8 bit) and double-head pulsed Nd:YAG laser (Beamtech Vlite 200, 532 nm, 7 ns pulse with 200 mJ) to illuminate the tracer particles. The cameras were equipped with lenses (Sigma 50mm DG MACRO) and narrow-band optical filters, which transmitted light scattered by the tracer particles at 532 nm (± 5 nm). The laser beam was converted into a laser sheet by using a system of cylindrical and spherical lenses. The OH PLIF consisted of a tunable pulsed dye laser (Sirah), pumped by a pulsed Nd:YAG laser (QuantaRay), and UV-sensitive ICCD camera (Princeton instruments PI-MAX-4, 16 bit), equipped with a UV-lens and band-pass optical filter. The average pulse energy of the tunable laser, excited $Q_1(8)$ line of the $A^2\Sigma–X^2\Pi$ (1–0) band, was approximately 5 mJ. The HCHO PLIF system consisted of a pulsed Nd:YAG laser Quantel Brilliant B (355 nm, 8 ns pulse with 50 mJ), UV-sensitive image intensifier (LaVision IRO) and sCMOS camera (LaVision, Imager sCMOS, 5 Mpix, 16 bit). The image intensifier was equipped with a UV-lens and band-pass filter.

A system of optical elements was used to organize illumination of the measurement plane (in the central cross-section) by laser sheets with thickness below 0.8 mm. The PLIF signal was collected almost in the middle of the time interval between two PIV laser pulses. In both cases the exposure time for each PLIF image was 200 ns. Time separation between two PIV laser pulses was 20 μs. An in-house ActualFlow software, developed in the Institute of Thermophysics, was used to acquire and process the data. The velocity fields were evaluated by an adaptive iterative cross-correlation algorithm with continuous image shift and deformation (for definition see Scarano 2001). The final size of the interrogation areas was 32×32 pixels. The spatial overlap rate between the neighbour interrogation areas was 50%. The spatial resolution of the PIV system corresponded to approximately 1 mm. A set of images post-processing algorithms was used to process the PLIF images to minimize effect of dark current and background luminosity, to correct for non-uniformity of the laser-sheet and spatial sensitivity of the sensors.

Spatial calibration of the stereo PIV and PLIF cameras was performed by using a plane calibration target and 3rd-order polynomial transforms. This was done by processing images of the calibration target placed in five different positions in the normal-to-plane direction with the step of 0.5 mm. In addition, to minimize the calibration error, an iterative correction procedure of possible misalignment between the laser sheet and the target plane was applied (Coudert and Schon, 2001). For almost entire measurement domain the mismatch between the actual locations of markers on the target and their coordinates in the obtained calibration models was below 1 pixel. To ensure that PIV and PLIF laser sheet planes were well aligned, a photo-sensitive paper was placed into the measurement volume and exposed to a single shot of each laser prior to the measurements.

3 Results

Figure 1 shows photographs of the unconfined flames and time-averaged PIV and PLIF data. For the low-swirl flow (S = 0.41) the flame is stabilized above the nozzle exit. According to the mean velocity

field, there is a wake zone formed downstream the nozzle exit inside the core of the expanding swirling jet. For the high-swirl flow (S = 1.0) there is a bubble-type central recirculation zone. The flame front is stabilized in the inner mixing layer between the annular swirling jet and central recirculation zone. The flame front penetrates inside the nozzle. Time-averaged OH PLIF signal reveals regions with hot combustion products, containing H_2O. On average. the HCHO PLIF reveals location of the chemical reaction zone, which has a shape similar to the visible flame front in the photographs.

Figures 2 and 3 shows flame images and time-averaged PIV and PLIF data for the swirling flame when the cold impingement surface is located at 3d and *1*d downstream the nozzle exit, respectively. For the case H = 3d the flame shapes are similar to those for the unconfined configurations. The main difference that for both swirl rates there are lengthy cone-like recirculation zones between the nozzle and the impingement plate. The PLIF data shows that OH fluorescence inside the recirculation zone is weak, which could be due to cooling of the reverse flow by the obstacle. Besides for the case of high swirl (S = 1.0), HCHO fluorescence occurs not only near the visible flame front, but also inside the recirculation zone. For H = 1d the separation distance is so small, that the flame front is deflected by the surface and spreads along it. According to the PIV data, cone-like recirculation zones are also present for both cases. On average, regions of OH and HCHO fluorescence have shape similar to that of the flame. For the high-swirl case, the HCHO fluorescence is weak inside the recirculation zone, as it is observed for the unconfined configuration.

In order to characterize coherent flow structures, the velocity data sets are processed by snapshot POD via singular value decomposition (SVD) method:

$$\mathbf{u}'(\mathbf{x},t_k)=\sum_{q=1}^{N}\alpha_q(t_k)\sigma_q\boldsymbol{\varphi}_q(\mathbf{x}), \tag{2}$$

$$\text{where } \frac{1}{M}\sum_{k=1}^{M}\boldsymbol{\varphi}_i(\mathbf{x}_k)\boldsymbol{\varphi}_j(\mathbf{x}_k)=\delta_{ij} \text{ and } \frac{1}{N}\sum_{k=1}^{N}\alpha_i(t_k)\alpha_j(t_k)=\delta_{ij} \tag{3}$$

The set of the fluctuating velocity fields [$\mathbf{u}'(\mathbf{x}, t_1)$...$\mathbf{u}'(\mathbf{x}, t_N)$] is represented as a finite series of the products of the spatial orthonormal basis functions $\boldsymbol{\varphi}_q$ with non-dimensional temporal coefficients α_q and singular values σ_q. N and M are the number of the snapshots in the set and number of spatial point in each snapshot, respectively. The singular values characterize amplitude (square root of the kinetic energy of the velocity fluctuations) of each POD mode. Their spectra are shown in Figure 4. It is found that the POD modes correspond to two different kinds of coherent structures. The examples are shown in Figure 5.

The first and second POD modes for the case H/d = 3 demonstrate two different kinds of coherent structures. The second POD mode is concluded to correspond to large-scale vortex structures formed in mixing layers of the jet. According the phase-averaged fluorescence intensity, they produce deformations of the reaction zone. In contrast, the first POD mode corresponds to large-scale flow oscillations during jet impingement onto the surface. According to the phase-averaged fluctuations of the HCHO PLIF signal, these large-scale flow motion are statistically correlated with variation of HCHO intensity inside the central recirculation zone.

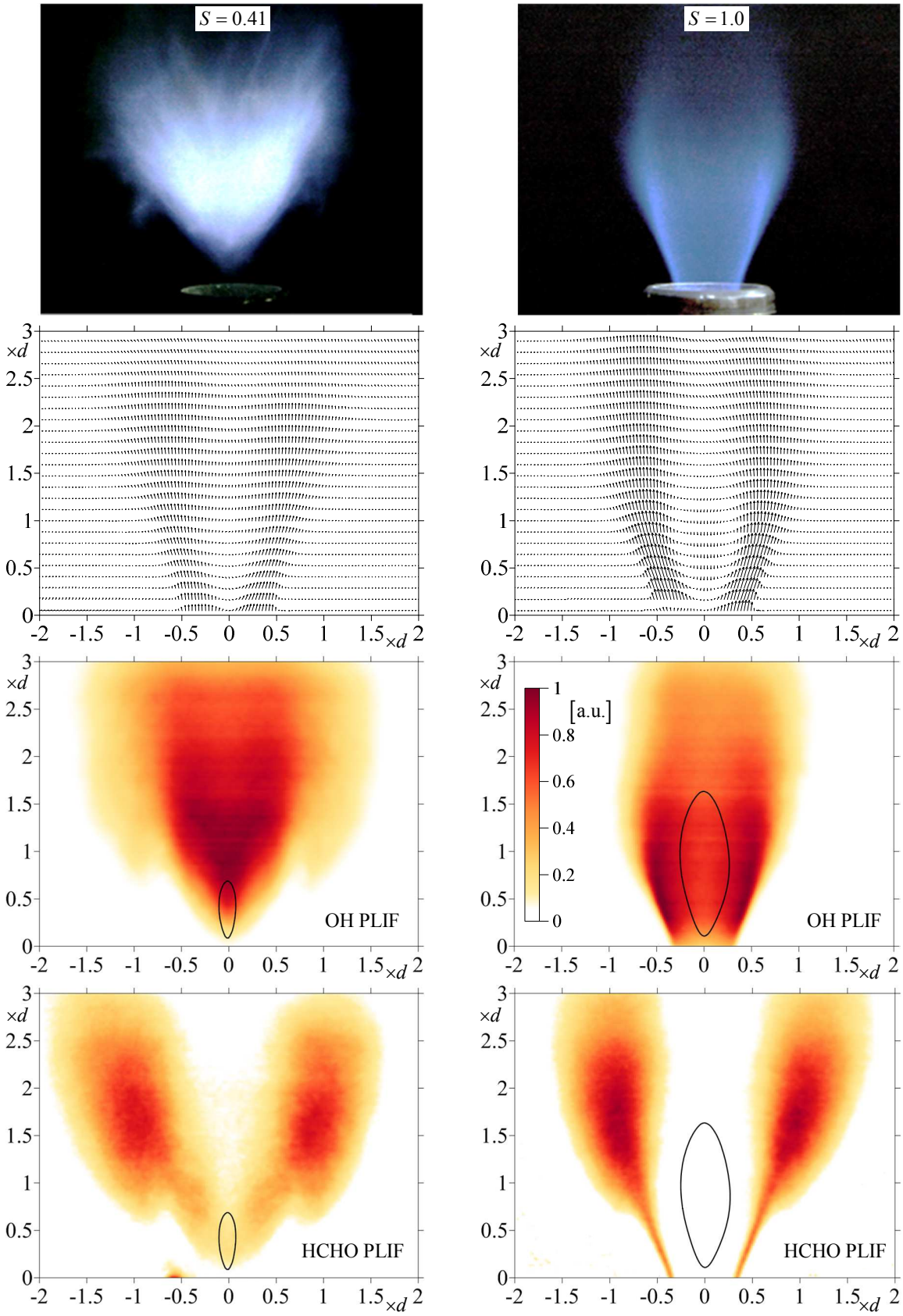

Figure 1: Photographs of unconfined flames and time-averaged PIV and PLIF data.

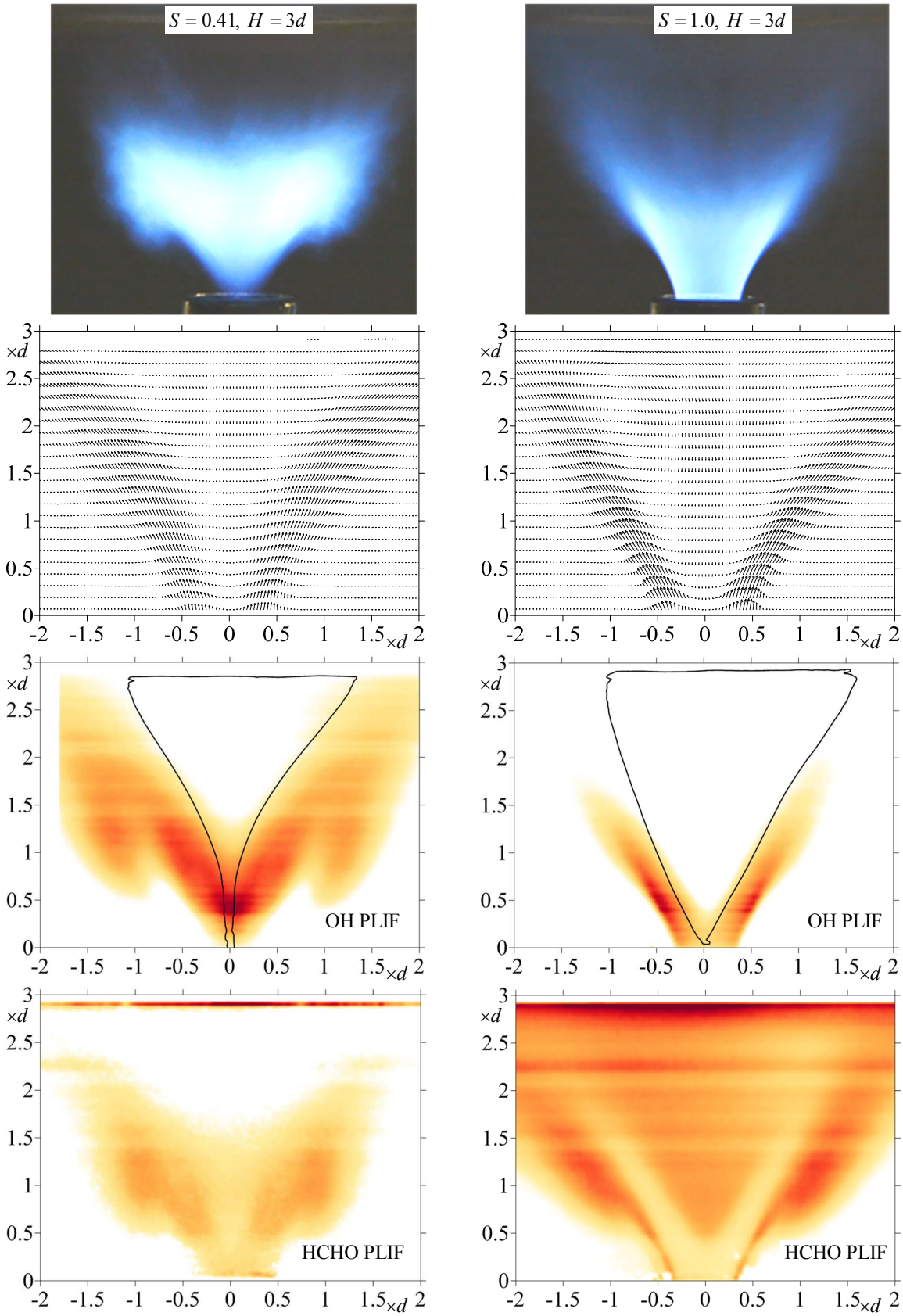

Figure 2: Photographs of impinging flames (H/d = 3) and time-averaged PIV and PLIF data.

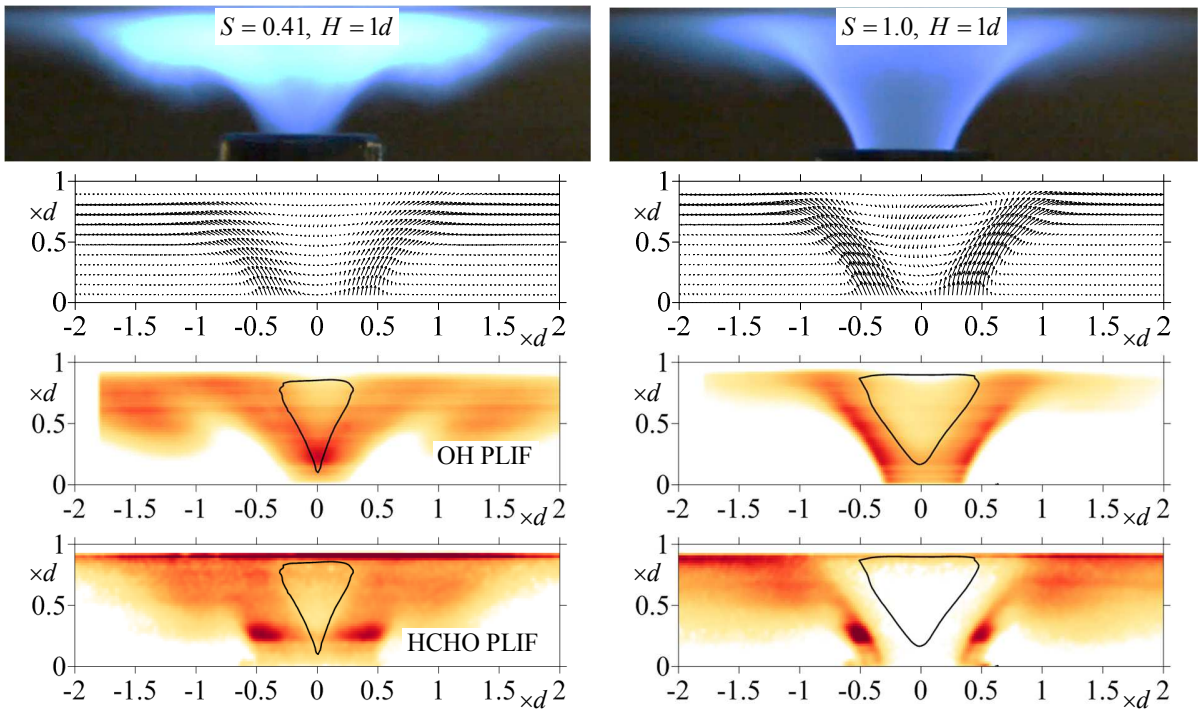

Figure 3: Photographs of impinging flames (H/d = 1) and time-averaged PIV and PLIF data.

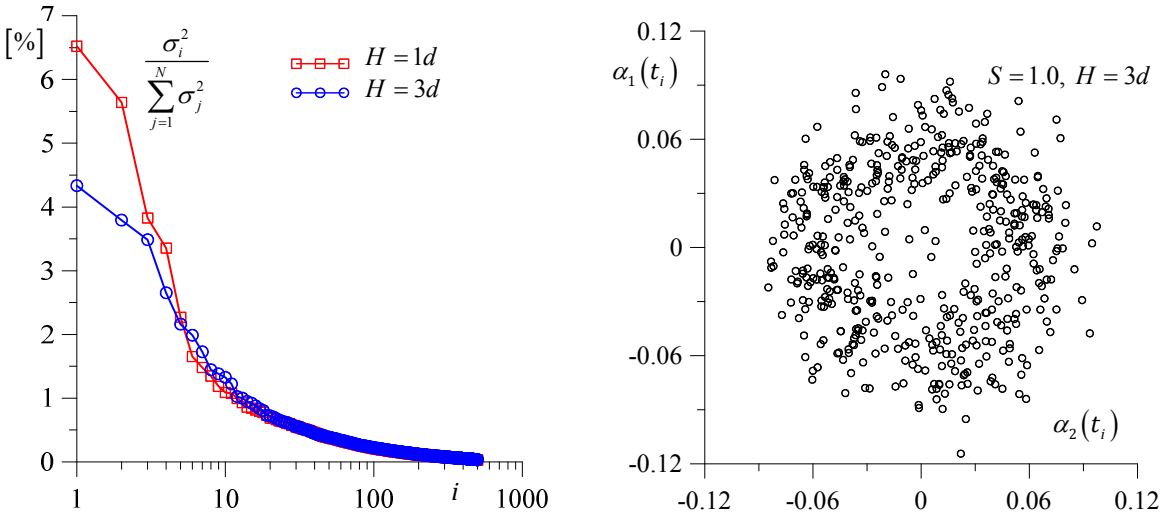

Figure 4: POD spectra for high-swirl flows (S = 1.0) and temporal coefficients for H/d=3.

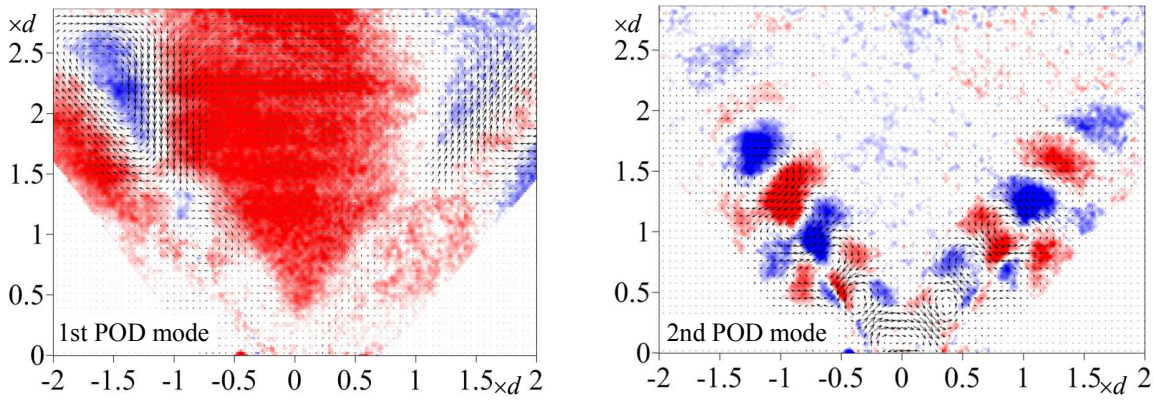

Figure 5: Spatial distributions of the first and second POD modes and corresponding phase-averaged fluctuations of the HCHO PLIF intensity for S = 1.0, H/d =3.

4 Conclusion

The performed combined study of coherent flow structures by PIV and flame front deformations by OH and HCHO PLIF in impinging swirling jets with premixed combustion has revealed two kinds of large-scale organized flow structures. One kind corresponds to vortex structures formed in the mixing layers of the jets. Another corresponds to large-scale flow oscillations during jet impingement onto the surface, statistically correlated with HCHO intensity inside the central recirculation zone.

Acknowledgements

The research is supported by the Russian Science Foundation (grant No 16-19-10566).

References

Alekseenko SV, Bilsky AV, Dulin VM, and Markovich DM (2007). Experimental study of an impinging jet with different swirl rates. *International Journal of Heat and Fluid Flow* 28(6): 1340-1359

Billant P, Chomaz JM, and Huerre P (1998). Experimental study of vortex breakdown in swirling jet. *Journal of Fluid Mechanics* 376:183-219

Chander S and Singh G (2013). Effect of Helical Vane Swirler Geometry on Heat Transfer Characteristics for Compressed Natural Gas/Air Swirling Flame Impinging on a Flat Surface. In *ASME 2013 International Mechanical Engineering Congress and Exposition* (pp. V08AT09A018-V08AT09A018). San Diego, California, USA, November 15–21

Cheng RK (1995). Velocity and scalar characteristics of premixed turbulent flames stabilized by weak swirl. *Combustion and Flame* 101: 1-14

Cheng RK, Littlejohn D, Nazeer WA, Smith K (2008). Laboratory studies of the flow field characteristics of low-swirl injectors for adaptation to fuel-flexible turbines. *Journal of Engineering for Gas Turbines and Power* 130: 021501

Coudert SJ and Schon JP (2001) Back-projection algorithm with misalignment corrections for 2D3C stereoscopic PIV. *Measurement Science and Technology* 12:1371–1381

Dreizler A and Böhm B (2015). Advanced laser diagnostics for an improved understanding of premixed flame-wall interactions. *Proceedings of the Combustion Institute* 35(1): 37-64

Edwards CF, Fornaciari NR, Dunsky CM, Marx KD, and Ashurst WT (1993). Spatial structure of a confined swirling flow using planar elastic scatter imaging and laser Doppler velocimetry. *Fuel* 72: 1151-1159

Fayoux A, Zähringer K, Gicquel O, and Rolon J (2005) Experimental and numerical determination of heat release in counterflow premixed laminar flames. *Proceedings of the Combustion Institute* 30: 251-257

Gupta AK, Lilley DG, and Syred N (1984) *Swirl flows*. Kent, U.K.: Abacus Press

Hassel EP and Linow S (2000). Laser diagnostics for studies of turbulent combustion. *Measurement Science and Technology* 11: R37-R57

Johnson MR, Littlejohn D, Nazeer WA, Smith KO, and Cheng RK (2005). A comparison of the flow fields and emissions of high-swirl injectors and low-swirl injectors for lean premixed gas turbines. *Proceedings of the Combustion Institute* 30:2867-2874

Kariuki J, Dowlut A, Yuan R, Balachandran R, and Mastorakos E (2015). Heat release imaging in turbulent premixed methane-air flames close to blow-off. *Proceedings of the Combustion Institute* 35: 1443-1450

Kohse-Höinghaus K. (1994). Laser techniques for the quantitative detection of reactive intermediates in combustion systems. *Progress in Energy and Combustion Science* 20: 203-279

Korobeinichev OP, Shmakov AG, Chernov AA, Markovich DM, Dulin VM, and Sharaborin DK (2014). Spatial and temporal resolution of the particle image velocimetry technique in flame speed measurements. *Combustion, Explosion, and Shock Waves* 50(5):510-517

Luo DD, Zhen HS, Leung CW, and Cheung CS (2010) Premixed flame impingement heat transfer with induced swirl. *International Journal of Heat and Mass Transfer* 53(19-20): 4333-4336

Miles RB, Lempert WR, Forkey JN (2001) Laser Rayleigh scattering. *Measurement Science and Technology* 12: R33-R51

Mulla IA, Dowlut A, Hussain T, Nikolaou ZM, Chakravarthy SR, Swaminathan N, and Balachandran R (2016). Heat release rate estimation in laminar premixed flames using laser-induced fluorescence of CH2O and H-atom. *Combustion and Flame* 165: 373-383

Oberleithner K, Sieber M, Nayeri CN, Paschereit CO, Petz C, Hege HC, Noack BR, and Wygnanski I (2011) Three-dimensional coherent structures in a swirling jet undergoing vortex breakdown: Stability analysis and empirical mode construction. *Journal of Fluid Mechanics* 679: 383–414

Röder M, Dreier T, and Schulz C (2012). Simultaneous measurement of localized heat release with OH/CH2O-LIF imaging and spatially integrated OH∗ chemiluminescence in turbulent swirl flames. *Applied Physics B* 107(3): 611-617

Scarano F (2001) Iterative image deformation methods in PIV. *Measurement Science and Technology* 13:R1–R19

Sharaborin DK, Markovich DM, and Dulin VM. (2018). Planar spontaneous Raman-scattering spectroscopy for reacting jet-flow diagnostics using Lyot–Ehman tunable filter. *Technical Physics Letters* 44: 53-56

Singh G, Chander S, and Ray A (2012) Heat transfer characteristics of natural gas/air swirling flame impinging on a flat surface. *Experimental Thermal and Fluid Science* 41: 165-176

Singh G and Chander S (2013). Effect of Swirl Intensity on Heat Transfer Characteristics of Swirling Flame Impinging on a Flat Surface. In *ASME 2013 International Mechanical Engineering Congress and Exposition* (pp. V08AT09A021-V08AT09A021). San Diego, California, USA, November 15–21

Singh S and Chander S (2014). Heat transfer characteristics of dual flame with outer swirling and inner non-swirling flame impinging on a flat surface. *International Journal of Heat and Mass Transfer* 77: 995-1007

Sirovich L (1987). Turbulence and the dynamics of coherent structures. I. Coherent structures. *Quarterly of Applied Mathematics* 45(3): 561-571

Stella A, Guj G, Kompenhans J, Raffel M, and Richard H (2001). Application of particle image velocimetry to combusting flows: design considerations and uncertainty assessment. *Experiments in Fluids* 30: 167-180

Syred N and Beer JM (1974) Combustion in swirling flows: a review. *Combustion and Flame* 23(2):143-201

Weber R and Dugué J (1992). Combustion accelerated swirling flows in high confinements. *Progress in Energy and Combustion Science* 18(4):349-367